Electronic Supplementary Material (ESI) for Journal of Materials Chemistry A.

Conjugated Polymer Electrodes Fabricated Using Rylene-Based Acceptors Toward High Energy and Power Density Symmetric Supercapacitor Operable in Organic Electrolyte Environment

Subir K. Pati[1], Dhananjaya Patra[1,], Sunita Muduli[2], Sabyashachi Mishra[2], Sungjune Park[1,*]*

[1]School of Chemical Engineering, Sungkyunkwan University, Suwon, Republic of Korea

[2]Department of Chemistry, Indian Institute of Technology, Kharagpur-721302, India

[*]Corresponding author email: itspilu@gmail.com, sungjunepark@skku.edu

1. EXPERIMENTAL DETAILS

1.1 Reagents and Materials

All chemicals and solvents were purchased in reagent grade from Aldrich, ACROS, and TCI, except the catalysts $Pd(PPh_3)_4$, and $Pd_2(dba)_2$ which were obtained from Strem Chemicals. Tetrahydrofuran was dried and purified by fractional distillation over sodium/benzophenone and handled in a moisture-free atmosphere. Chlorobenzene was used for the polymerization was received from Aldrich which is protected by sure seal paced with N_2. Purification of the intermediates by column chromatography techniques using silica gel (Merck, Kieselgel 60 63-200 MYM SC). The monomers M1 [S1] were synthesized by our group previously presented in scheme 1 and other two monomers M2 [S2] and M3 [S3], were synthesized by a slightly modified procedure as reported in the literatures.

1.2 General information - Equipment and procedural details

1.2.1 Nuclear magnetic resonance spectroscopy (NMR)

^1H and ^{13}C NMR spectra were recorded from $CDCl_3$ solutions using a Bruker AVANCE 400 MHz spectrometer at a temperature of 298 K; chemical shifts are reported as δ values (ppm), for 1H-NMRs referenced to the residual solvent peaks (δ: 7.26 for $CDCl_3$) and ^{13}C-NMRs, spectra were referenced to the residual solvent peaks (δ: 77.16 for $CDCl_3$).

1.2.2 Thermogravimetric analysis (TGA)

The thermogravimetric analysis (TGA) was conducted by Q400 (WATERS, USA) for all the co-polymers which exhibited high thermal stability and the thermal decomposition temperature (T_d) at 5% weight loss are all above 350 °C.

1.2.3 Gel permeation chromatography (GPC)

Gel permeation chromatography (GPC) was obtained from the Waters (Alliance e2695) model to determine the molecular weights of both the copolymers.

1.2.4 Ultraviolet-visible spectroscopy

UV–Vis absorption spectra were recorded using Hewlett Packard (mode: HP 8453) absorption spectrometer from dilute solutions in chloroform or from solid films that had been spin-coated onto glass substrate from dilute chloroform solutions (5 mg mL^{-1}).

1.2.5 Cyclic voltammetry for energy levels measurement

The electrochemical measurements were carried out in a deoxygenated solution of 0.1 M tetra-n-butylammoniumhexafluorophosphate ($TBAPF_6$) in acetonitrile with a computer-controlled electrochemical workstation (Amtek VersaSTAT 3 instrument (AMETEK Scientific, USA)). A glassy carbon electrode, a Pt wire, and an Ag/AgCl electrode were used as the working, counter, and reference electrodes, respectively. The corresponding energy levels of the highest occupied molecular orbital (HOMO) and lowest unoccupied molecular orbital (LUMO) were calculated from the experimental values of $E_{ox/onset}$ and $E_{red/onset}$ for the solid films **BT-NDI** and **BT-PDI**, formed by drop-casting films at a similar thickness (ca. 5 mg mL^{-1} in chloroform). The onset potentials were determined from the intersections of two tangents drawn at the rising currents and background currents of the CV measurements.

1.2.6 X-ray diffraction (XRD)

XRD measurement of the polymer powders were conducted on a Bruker D8 Powder diffractometer using Cu X-ray tube (2.2 KW) with maximum voltage 40 kV and power 40 mA in with the 2θ of 3° to 30°.

1.2.7 Field emission scanning electron microscopy (FESEM)

Field emission type scanning electron microscope (FE-SEM, Hitachi, S-4700) was used for the morphology analysis of the powder polymeric samples.

1.2.8 Field Emission transmission electron microscopy (FETEM)

The elemental mapping and distribution of individual elements (Wt% and Atomic %) was calculated from the EDS mapping taken JEOL (JEM-ARM200F) Cs corrected-Field Emission Transmission Electron Microscope.

2. Computational Details

The ground state geometries of the BT-based conducting oligomers (monomer to trimer) i.e., **BT-NDI** and **BT-PDI** featuring dual acceptor moieties were optimized to understand their electronic properties by employing the density functional theory [S4] (DFT) method with the 6-31G(d, p)[S5,S6] basis set and the B3LYP[S7] functional along with the polarized continuum (PCM) model of implicit solvation. The TD-DFT calculations were performed at the same level of theory and with the CAM-B3LYP [S8] functional. The shorter and longer alkyl substituents of the polymer structure were replaced by methyl and ethyl groups, respectively for the simplification purpose. The vibrational frequencies were identified by performing Hessian calculations on the stationary points attained after achieving self-consistent field convergence. The wave functions extracted from the Gaussian 16 software [S9] were utilized to analyze the frontier molecular energy levels and band gap of the oligomers, whereas NTO and MESP analyses were conducted using the Multiwfn 3.8[S10] and VMD software 1.9.1.[S11]

3. Electrochemical measurements

3.1 Electrode Fabrication

All electrochemical measurements were conducted using an Amtek VersaSTAT 3 instrument (AMETEK Scientific, USA). The slurry for the working electrode was prepared by mixing the polymeric electrode materials (**BT-NDI** and **BT-PDI**, respectively), conducting carbon black and polyvinylidene difluoride (PVDF) binder with a weight ratio of 75:15:10, using 1,2-dichlorobenzene (DCB) as the solvent. The working electrodes were prepared by drop casting method over pre-activated carbon cloth (CC) substrates with a mass loading of approximately 2 mg/cm^2.

3.2 Formulas used

The specific capacitance was calculated from the GCD curves using Equation S1:

$$Cs = \frac{(I \times \Delta t)}{(m \times \Delta V)} \quad \text{(S1)}$$

where Cs, I/m, Δt, and ΔV denote the specific capacitance (F g^{-1}), applied current density (A g^{-1}), discharge time (s), and potential window of the charge–discharge curve, respectively.

For a symmetric supercapacitor device, multiplication by a factor of two (specific capacitance contribution from both electrodes) in SI Equation 1 is performed considering the mass loading of both the electrodes in the single cell used, as shown in Equation S2:

$$Cs = 2 \times \frac{(I \times \Delta t)}{(m \times \Delta V)} \quad \text{(S2)}$$

The energy density, E, and power density, P, of the two-electrode systems are calculated using Equation S3 and S4.

$$\text{Energy density (Wh kg}^{-1}) = \frac{Cs(\Delta V)^2}{7.2} \quad \text{(S3)}$$

$$\text{Power density (W kg}^{-1}) = \frac{E}{\Delta t \times 3600} \quad \text{(S4)}$$

Scheme 1. Synthetic routes of the monomers (M1–M3)

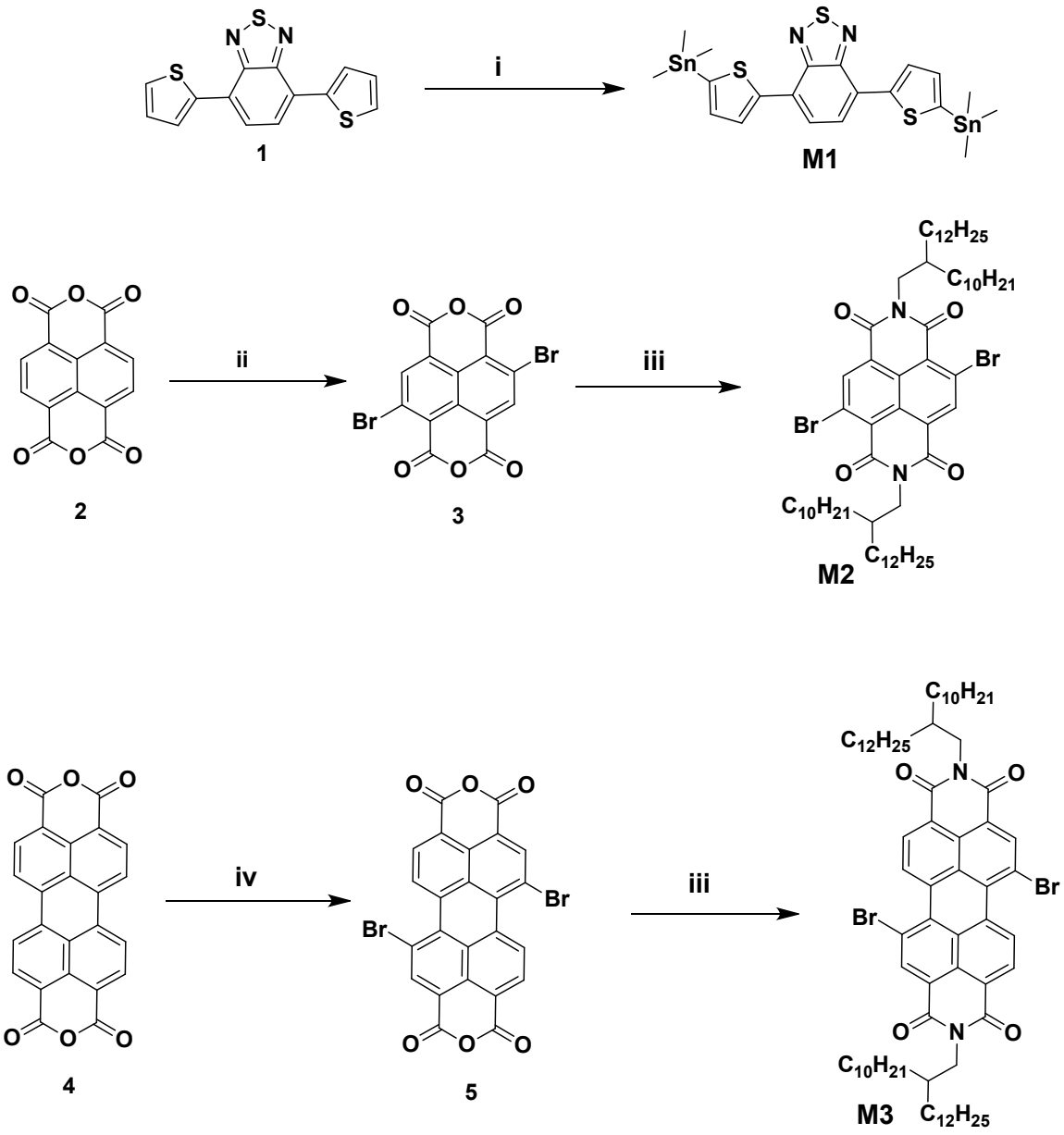

Reagents and conditions: (i) THF, n-BuLi, -78 °C, 2,2,6,6-tetramethylpiperidine (TMP) (ii) DBI, oleum, (iii) 2- 2-decyltetradecan-1-amine, o-Xylene, Propionic Acid, 140 °C; (iv) Br_2, H_2SO_4, 85 °C.

Scheme 2. Synthesis of BT-diimidie based polymers (BT-NDI and **BT-PDI)**

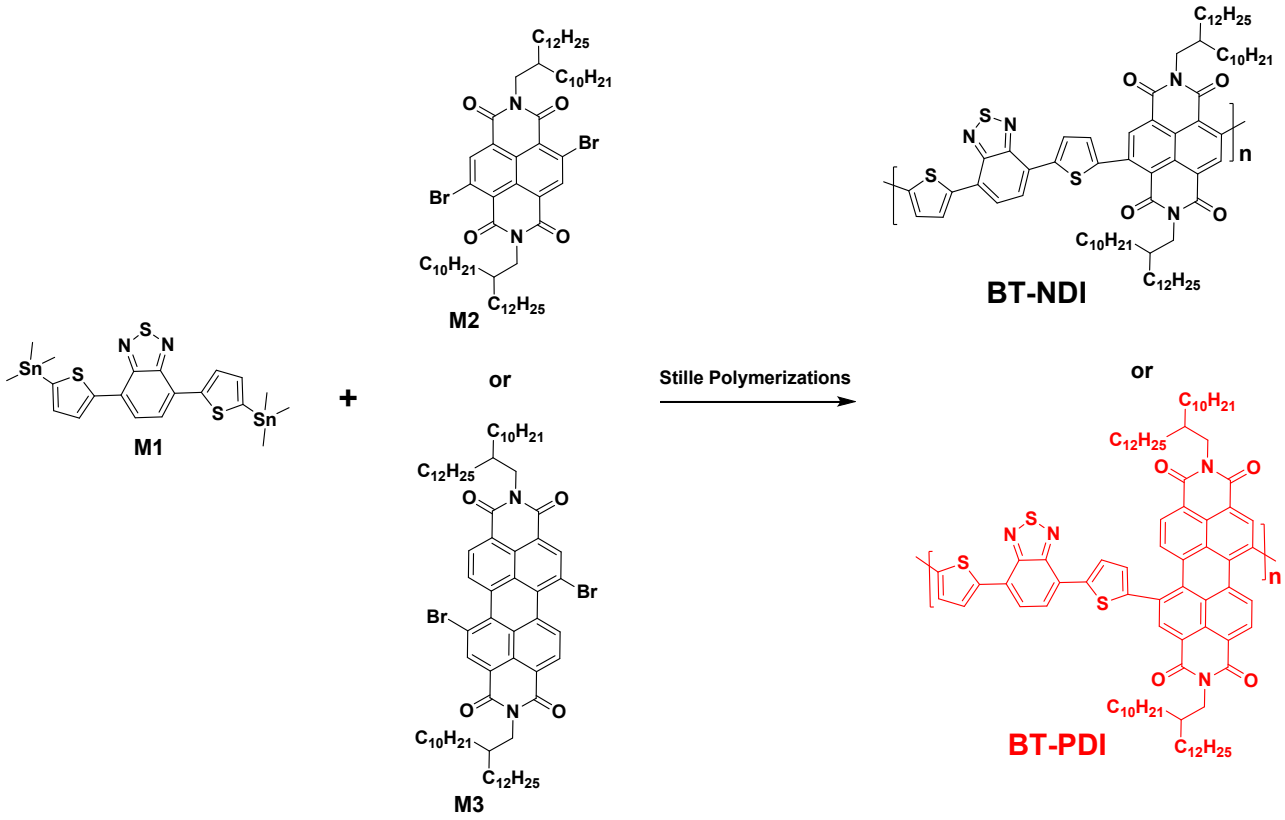

Stille polymerization conditions: P(*o*-tolyl)$_3$, CuI, $Pd_2(dba)_3$, and chlorobenzene at 130 °C for 24 hr.

Synthesis of monomers

N,N'-bis(2-decyltetradecyl)-2,6-dibromonaphthalene-1,4,5,8- bis(dicarboximide) (M2)

To a flame dried a two neck round bottom flask charged compound 3 (2.0 g, 4.69 mmol), 2- 2-decyltetradecan-1-amine[x] (4.98 g, 14.08 mmol), o-xylene (1 mL), and propionic acid (5 mL), the resulting mixture was stirred at 140 °C for 2 h. After cooling to room temperature, the solvents were removed in vacuo, and the residue was purified by column chromatography on silica gel with a mixture of chloroform:hexane (1:2, v/v) as eluent. The resulting product was a slight yellow solid with a yield of 1.95 g, 38%. ^{1}H-NMR (400 MHz, $CDCl_3$, δ) 8.98 (s, 2H), 4.14 (d, J = 4 Hz, 2H), 1.98 (m, 2H), 1.48-1.22 (m, 68H), 0.88-0.84 (m, 12H). ^{13}C-NMR (100 MHz, $CDCl_3$, δ) 161.18, 161.03, 139.17, 128.38, 127.25, 125.29, 124.08, 45.45, 36.47, 31.93, 31.55, 30.04, 29.70, 29.67, 29.66, 29.61, 29.38, 29.36, 26.34, 22.70, 14.14. Elemental analysis calculated for [$C_{62}H_{100}Br_2N_2O_4$]: C, 67.86; H, 9.19; N, 2.55. Obtained: C, 67.52; H, 9.10, N, 2.52.

5,12-dibromo-2,9-bis(2-decyltetradecyl)anthra[2,1,9-def:6,5,10-d'e'f']diisoquinoline-1,3,8,10(2H,9H)-tetraone (M3)

To the mixture of compound 4 (2.1 g, 3.81 mmol), 2- 2-decyltetradecan-1-amine[x] (4.05 g, 11.45 mmol), o-xylene (12 mL), and propionic acid (4 mL) was stirred in a two neck round bottomed flask at 140 °C for 2 h. Later in the reaction was cooling to room temperature, the solvents were removed in vacuo, and the residue was purified by column chromatography on silica gel with a mixture of chloroform:hexane (1:1, v/v, gradually up to 3:2) as eluent, resulting a red solid powder (0.63 g, 1.91 mmol, yield 74.7%). ^{1}H-NMR (400 MHz, $CDCl_3$, δ) 9.49 (d, J = 8.0 Hz, 2H), 8.87 (s, 2H), 8.65 (d, J = 8.0 Hz, 2H), 4.12 (d, J = 7.2 Hz, 4H), 2.0-1.98 (m, 2H), 1.57-1.30 (m, 68H), 0.86-0.82 (m, 12H). ^{13}C-NMR (100 MHz, $CDCl_3$, δ) 163.18, 16.69, 1338.06, 132.86, 130.02, 129.20, 128.44, 126.95, 123.18, 122.75, 120.81, 44.89, 36.68, 31.91, 31.88, 31.76, 31.72, 30.05, 29.74, 29.59, 29.32, 26.51, 26.50, 22.67, 14.11. Elemental analysis calculated for [$C_{72}H_{104}Br_2N_2O_4$]: C, 70.80; H, 8.58; N, 2.29. Obtained: C, 70.72; H, 8.51; N, 2.21.

General procedure for the synthesis of BT-NDI/PDI-based polymers:

A 20 mL clean and dry microwave vial was charged with monomer M1, monomer M2 (0.150 mmol), or M3 (0.150 mmol), $Pd_2(dba)_3$ (0.005 g, 0.005 mmol), P(*o*-tolyl)$_3$ (0.006 g, 0.02 mmol), and CuI (0.004 g, 0.02 mmol). The sealed microwave vial was subjected to three cycles of vacuum and purged with N_2, followed by the addition of chlorobenzene (5 mL) at 130 °C for 24 h. After cooling to room temperature, the reaction mixture was added dropwise to a mixture of hydrochloric acid (1 N, 10 mL) and methanol (200 mL), and stirred for 2 h. The polymer precipitate was filtered through a thimble and purified by Soxhlet extraction with methanol, acetone, hexane, dichloromethane, and chloroform for 24 h. The chloroform-soluble fraction was concentrated and reprecipitated into methanol, filtered, and dried under a vacuum to obtain the desired polymers as dark solid powders.[S12]

BT-NDI *Poly-{2,7-bis(2-decyltetradecyl)-4-methyl-9-(5-(7-(5-methylthiophen-2-yl)benzo[c][1,2,5]thiadiazol-4-yl)thiophen-2-yl)benzo[lmn][3,8]phenanthroline-1,3,6,8(2H,7H)-tetraone}*: Using monomer M1 (94 mg), M2 (164 mg), yield: 123.3 mg, 65%, GPC: Mw = 24.9 K Da, Đ = 1.68.

BT-PDI *Poly-{2,9-bis(2-decyltetradecyl)-5-methyl-13-(5-(7-(5-methylthiophen-2-yl)benzo[c][1,2,5]thiadiazol-4-yl)thiophen-2-yl)anthra[2,1,9-def:6,5,10-d'e'f']diisoquinoline-1,3,8,10(2H,9H)-tetraone}*: using monomer M1 (94 mg) and M3 (183 mg), yield: 130 mg, 71% GPC: Mw = 39.5 K Da, Đ = 1.66.

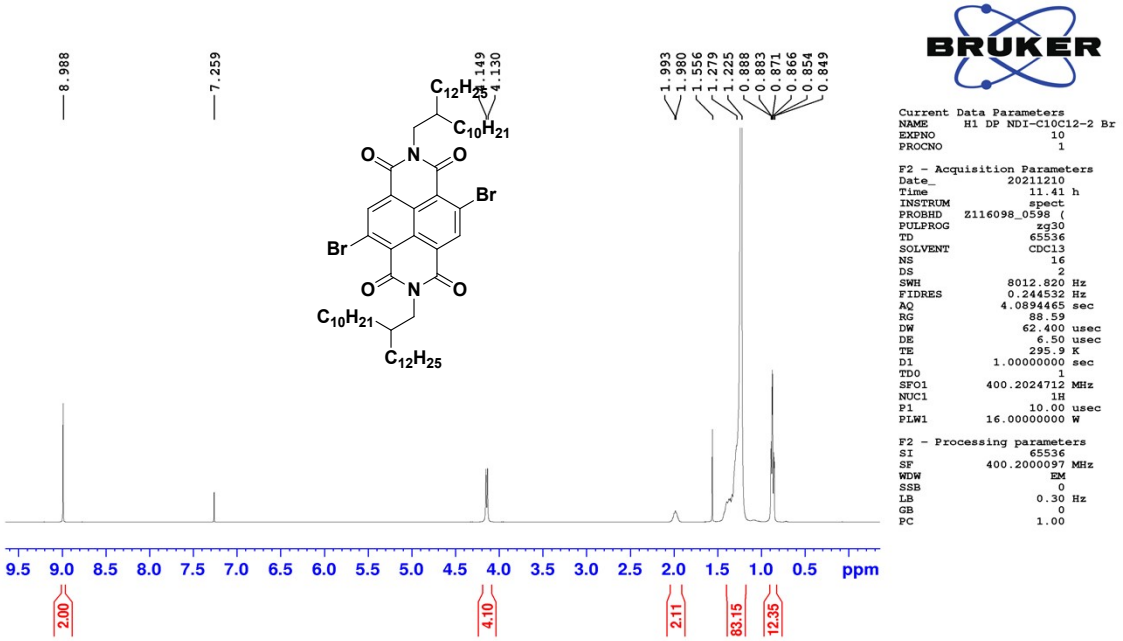

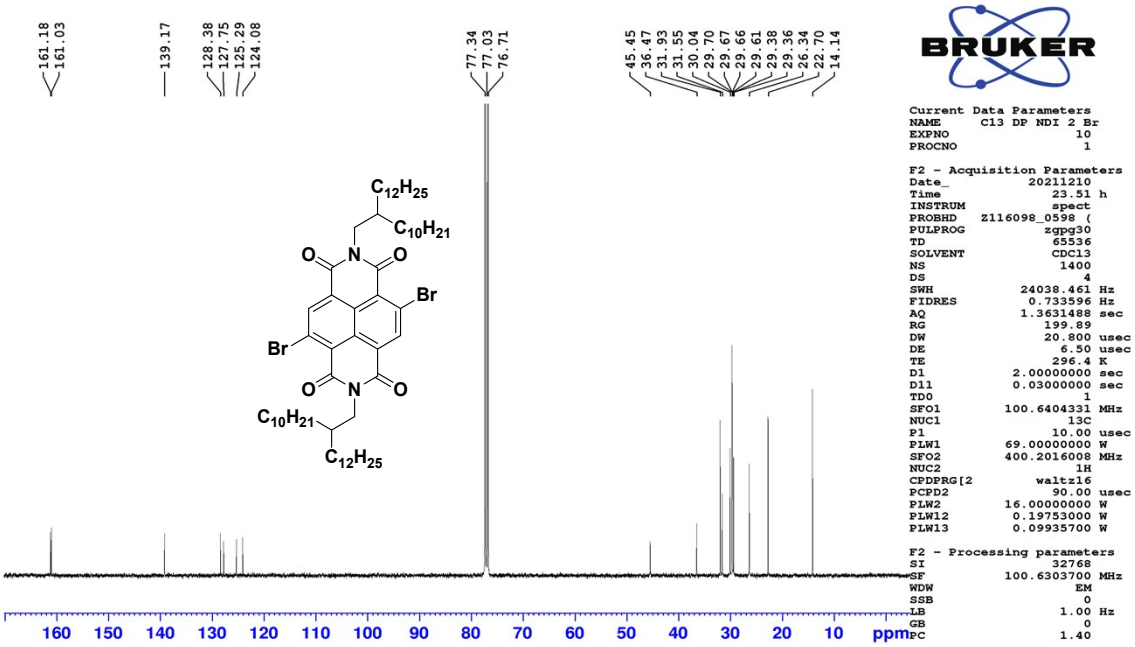

Supplementary Figure S1. ^{1}H- and ^{13}C-NMR spectra of monomer M2 in $CDCl_3$.

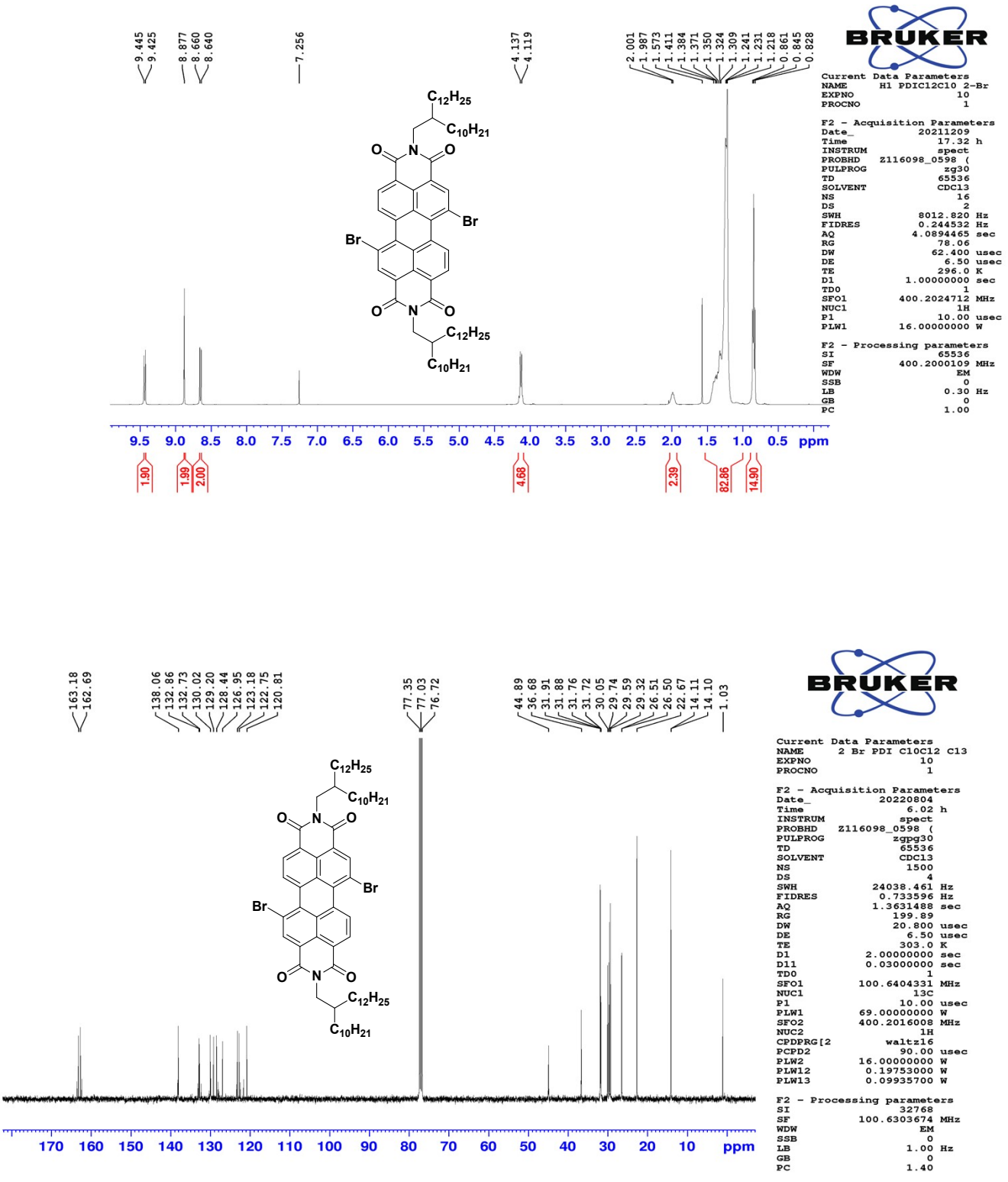

Supplementary Figure S2. ^{1}H- and ^{13}C-NMR spectra of monomer M3 in $CDCl_3$.

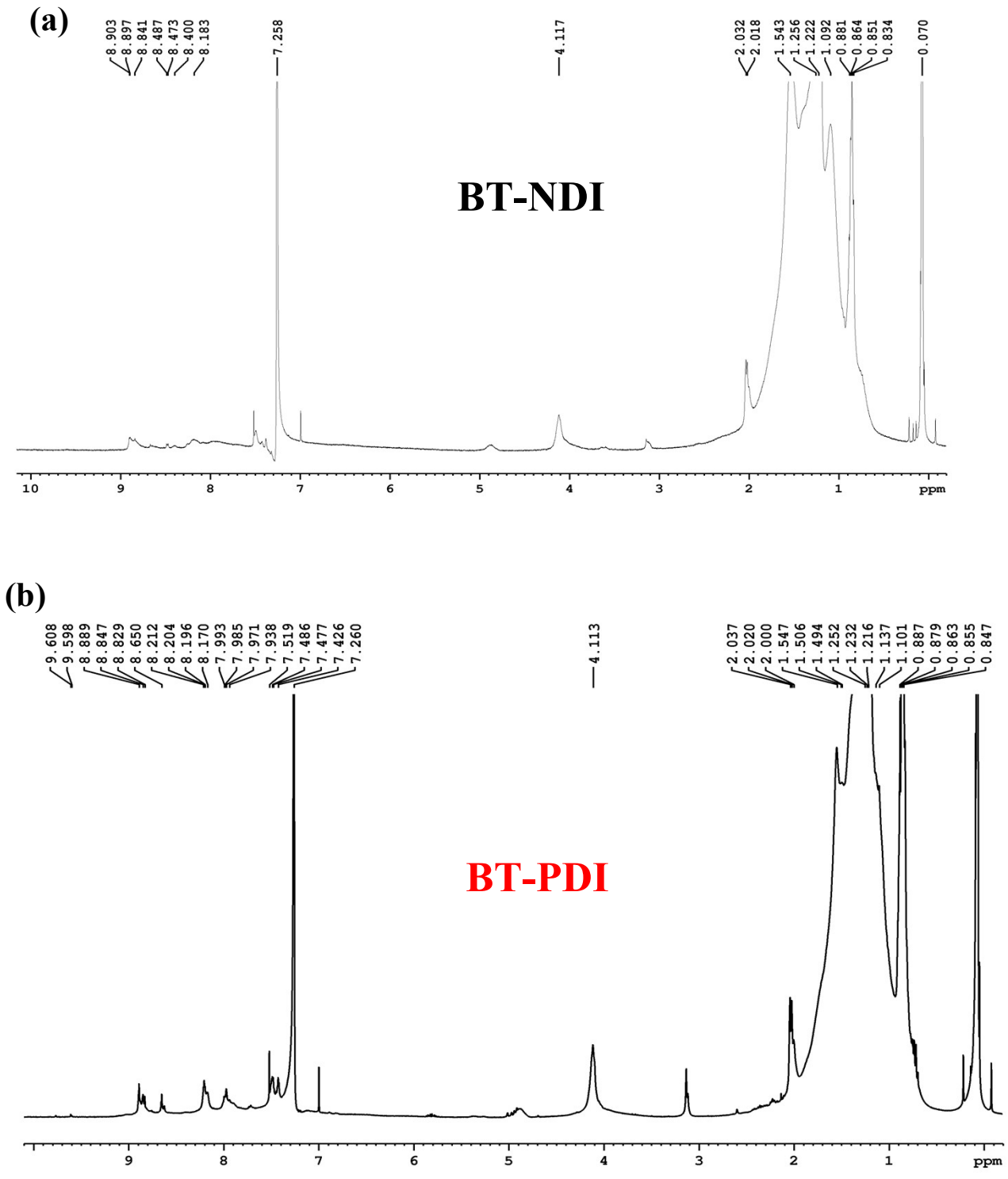

Supplementary Figure S3. 1H- NMR spectra of Polymer (a) **BT-NDI** and (b) **BT-PDI** $CDCl_3$.

Empower™ 3 SOFTWARE

GPC

SAMPLE INFORMATION

Sample Name:	BT-NDI	Acquired By:	System
Sample Type:	Broad Unknown	Sample Set Name:	240229
Vial:	22	Acq. Method Set:	Test
Injection #:	1	Injection Volume:	100.00 ul
Run Time:	50.0 Minutes	Date Acquired:	3/1/2024 9:35:58 AM KST

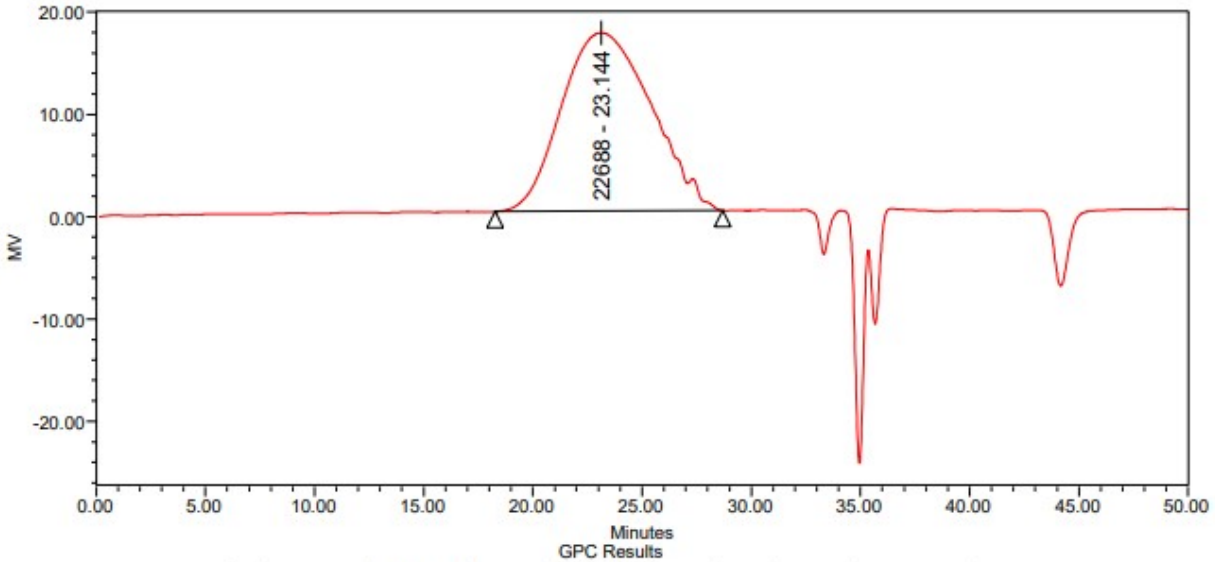

GPC Results

	Dist Name	Retention Time (min)	% Area	% Height	Mn	Mw	MP	Polydispersity
1		23.144	100.00	100.00	14825	24906	22688	1.680010

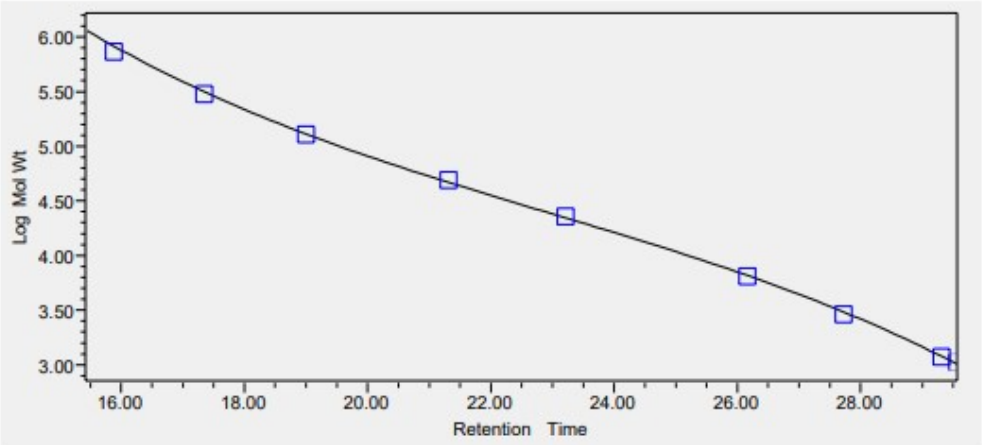

Supplementary Figure S4.(a) Gel permeation chromatography (GPC) molecular weight (M_w) of the copolymer **BT-NDI**

Empower™3 SOFTWARE

GPC

SAMPLE INFORMATION

Sample Name:	BT-PDI	Acquired By:	System
Sample Type:	Broad Unknown	Sample Set Name:	240229
Vial:	23	Acq. Method Set:	Test
Injection #:	1	Injection Volume:	100.00 ul
Run Time:	50.0 Minutes	Date Acquired:	3/1/2024 10:27:13 AM KST

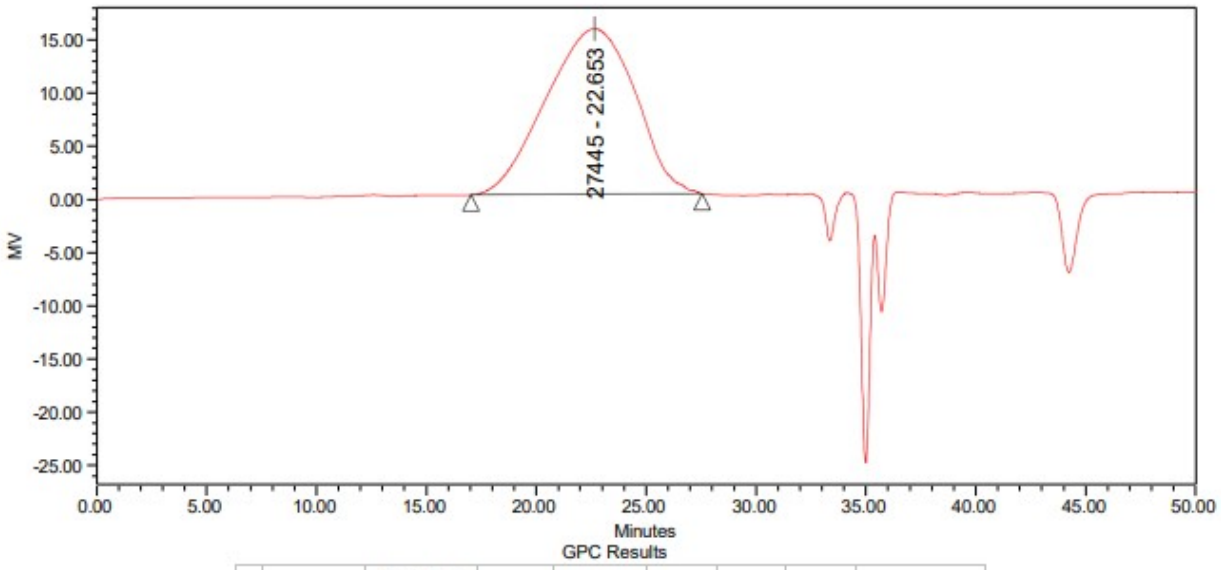

GPC Results

	Dist Name	Retention Time (min)	% Area	% Height	Mn	Mw	MP	Polydispersity
1		22.653	100.00	100.00	23745	39547	27445	1.665483

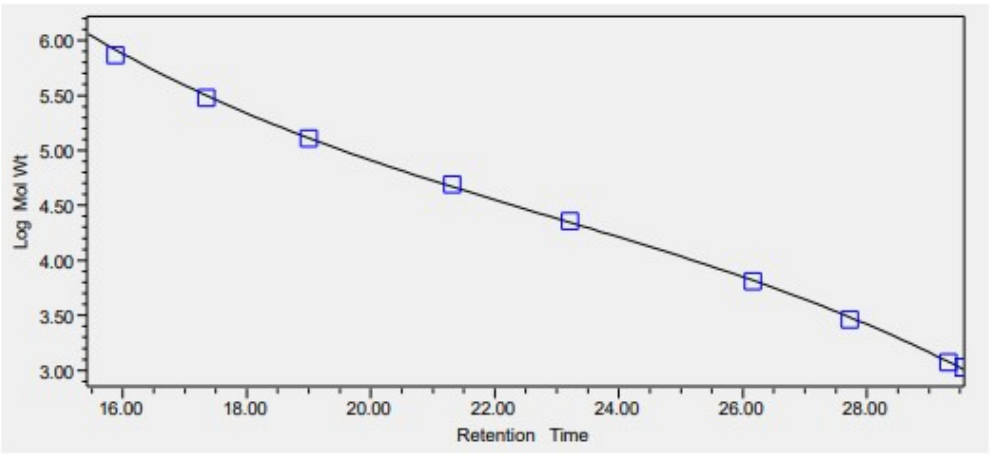

Supplementary Figure S4.(b) Gel permeation chromatography (GPC) molecular weight (M_w) of the copolymer **BT-PDI**

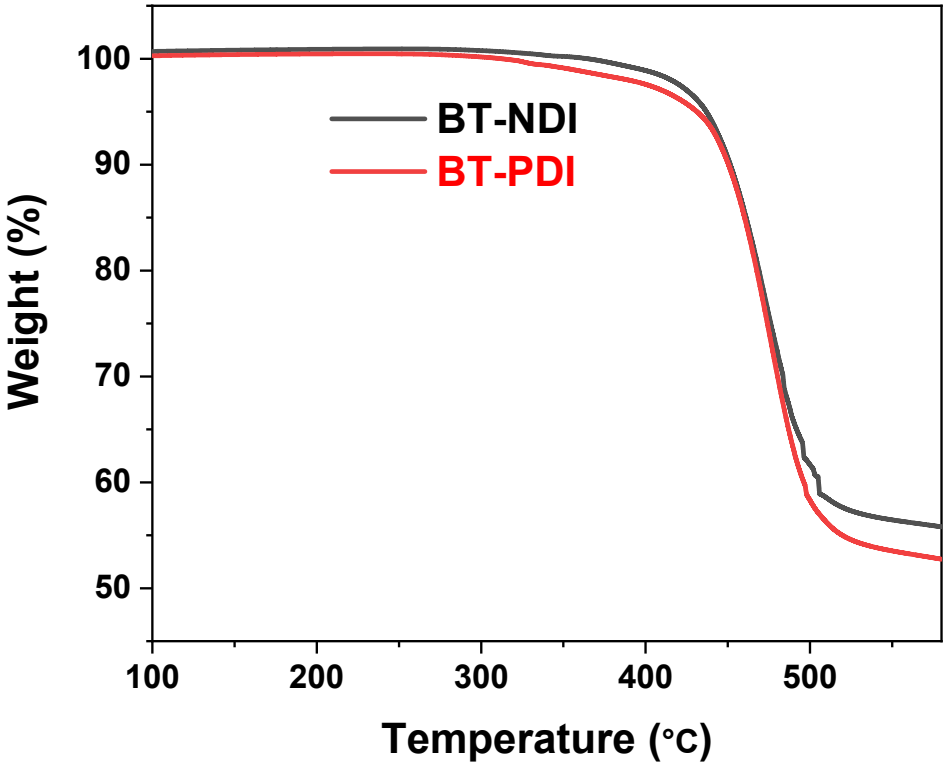

Supplementary Figure S5. TGA thermograms of copolymers **BT-NDI**, and **BT-PDI** under N_2 flow at 10 °C min^{-1}.

Supplementary Table T1. Summary of literature survey on similar types of n-type polymer based supercapacitor materials (3-electrode system)

Electrode	Electrolyte	Operating Voltage	Current Density / Scan Rate	Specific Capacitance	Cyclic Stability (%)	Reference - Year
rGO-NDI	1 M H_2SO_4	–0.5 to 0.5	5 mV s^{-1}	354 F g^{-1}	-	25 - 2021
rGO/NDI-CN	1 M H_2SO_4	0 to 1.2	0.5 A g^{-1}	336 F g^{-1}	10000 cycles 80% @ 10 A g^{-1}	26 - 2022
P(PDI-alt-BDT)	1 M $LiClO_4$/propylene carbonate	-1 to 1	0.5 Ag^{-1}	113 F g^{-1}	-	27 - 2019
PEDOT/PDI	0.1 M $TBAPF_6$	0 to 1 0 to -1	0.5 Ag^{-1}	78.6 F g^{-1} 73.1 F g^{-1}	1000 cycles (80%)	28 - 2020
NDI-Th/GF	1 M H_2SO_4	-0.2 to 1	0.5 Ag^{-1}	173.33 F g^{-1}	3000 cycles 82% @ 2 A g^{-1}	29 - 2024
P(NDI2OD-OThPV) (DHRP)	0.5 M H_2SO_4	–0.7 to 0.5	0.5 A g^{-1}	124 F g^{-1}	5000 cycles 100% @ 5 A g^{-1}	42 - 2018
BT-PDI	**0.1 M $TBAPF_6$**	**-1.5 to 0**	**1 A g^{-1}**	**196 F g^{-1}**	**5000 Cycles 76.2% @ 5 A g^{-1}**	**This study**

Supplementary Table T2.

(a) Distribution of individual elements (Wt% and Atomic %) from HRTEM EDS

Project 1 19/05/2023

Map Sum Spectrum							
Element	Line Type	k Factor	k Factor type	Absorption Correction	Wt%	Wt% Sigma	Atomic %
C	K series	2.512	Theoretical	1.00	83.31	0.70	88.75
N	K series	3.166	Theoretical	1.00	4.30	0.69	3.93
O	K series	1.869	Theoretical	1.00	5.93	0.30	4.75
S	K series	0.959	Theoretical	1.00	6.45	0.21	2.58
Total:					100.00		100.00

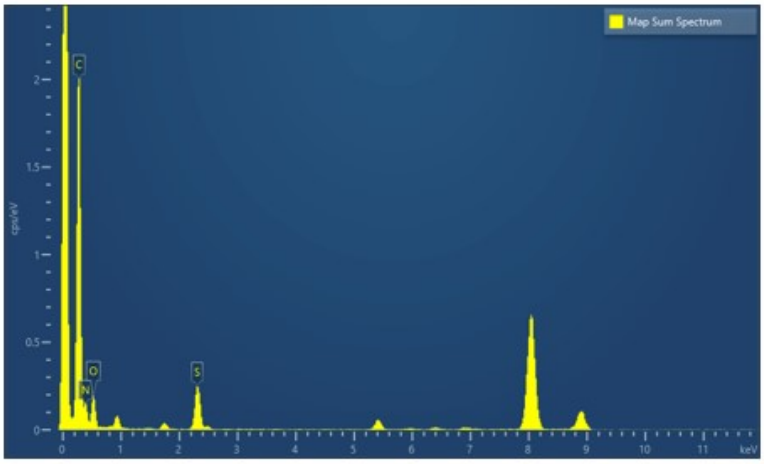

OXFORD INSTRUMENTS
The Business of Science®

(b) Comparison of distribution of individual elements (Atomic %) from HRTEM EDS and Calculation

		C	N	O	S	H
BT-PDI $C_{88}H_{116}N_4O_4S_3$	**From EDS**	**88.75 %**	**3.93 %**	**4.75 %**	**2.58 %**	
	Calculated	**76.03 %**	**4.03 %**	**4.6 %**	**6.92 %**	**8.41 %**

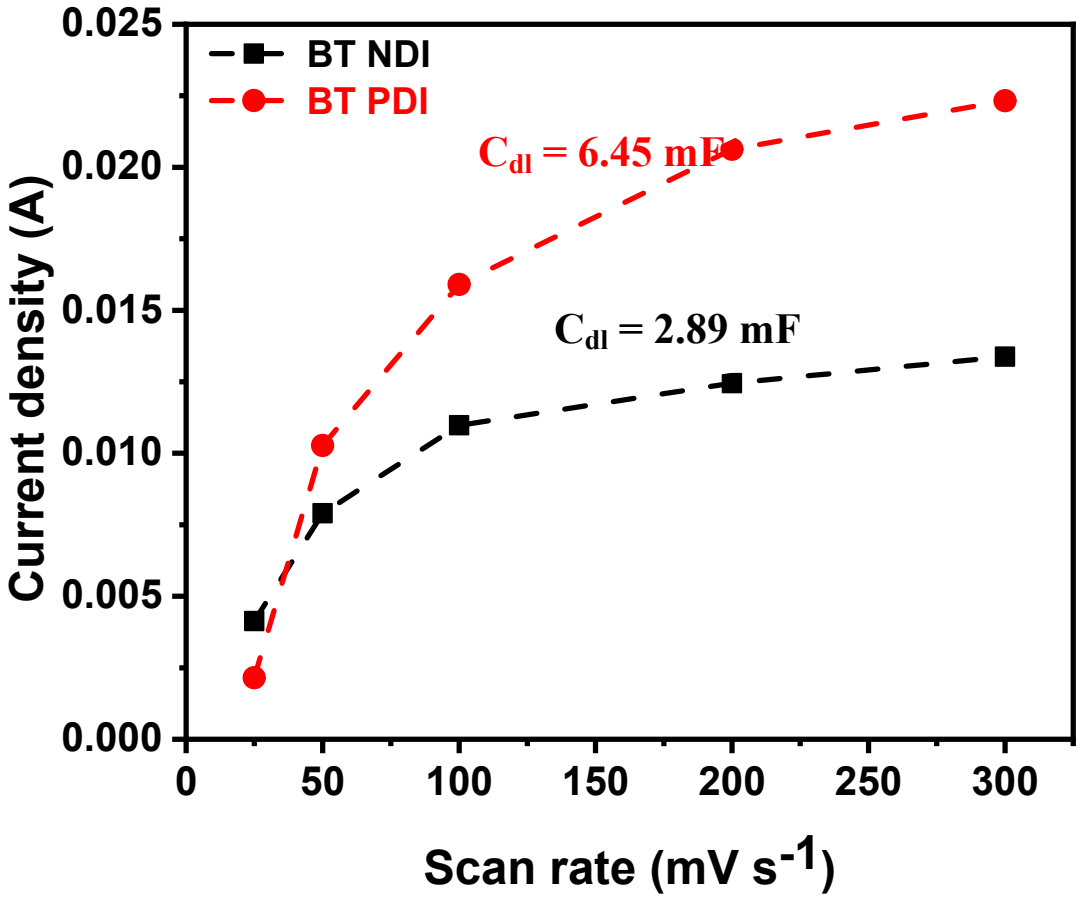

Supplementary Figure S6. The C_{dl} values for ECSA study, showing the corresponding linear fits of **BT-NDI** and **BT-PDI** in the range of 0 to -0.1 V CV.

The electrochemical double-layer capacitance (C_{dl}) for the working electrodes was characterized to calculate electrochemically active surface area (ECSA), determining the active redox reaction region. The C_{dl} of **BT-PDI** is 6.45 mF, which is higher than that of **BT-NDI** electrode (2.89 mF), indicating the presence of numerous beneficial active sites at the electrode-electrolyte interfaces, which enable the electrode to achieve better supercapacitive performance. The ECSA values for **BT-NDI** and **BT-PDI** was calculated to be 72.25 and 161.46 cm^2, respectively using following equation.[S13]

$$ECSA = C_{dl}/C_s \quad (S5)$$

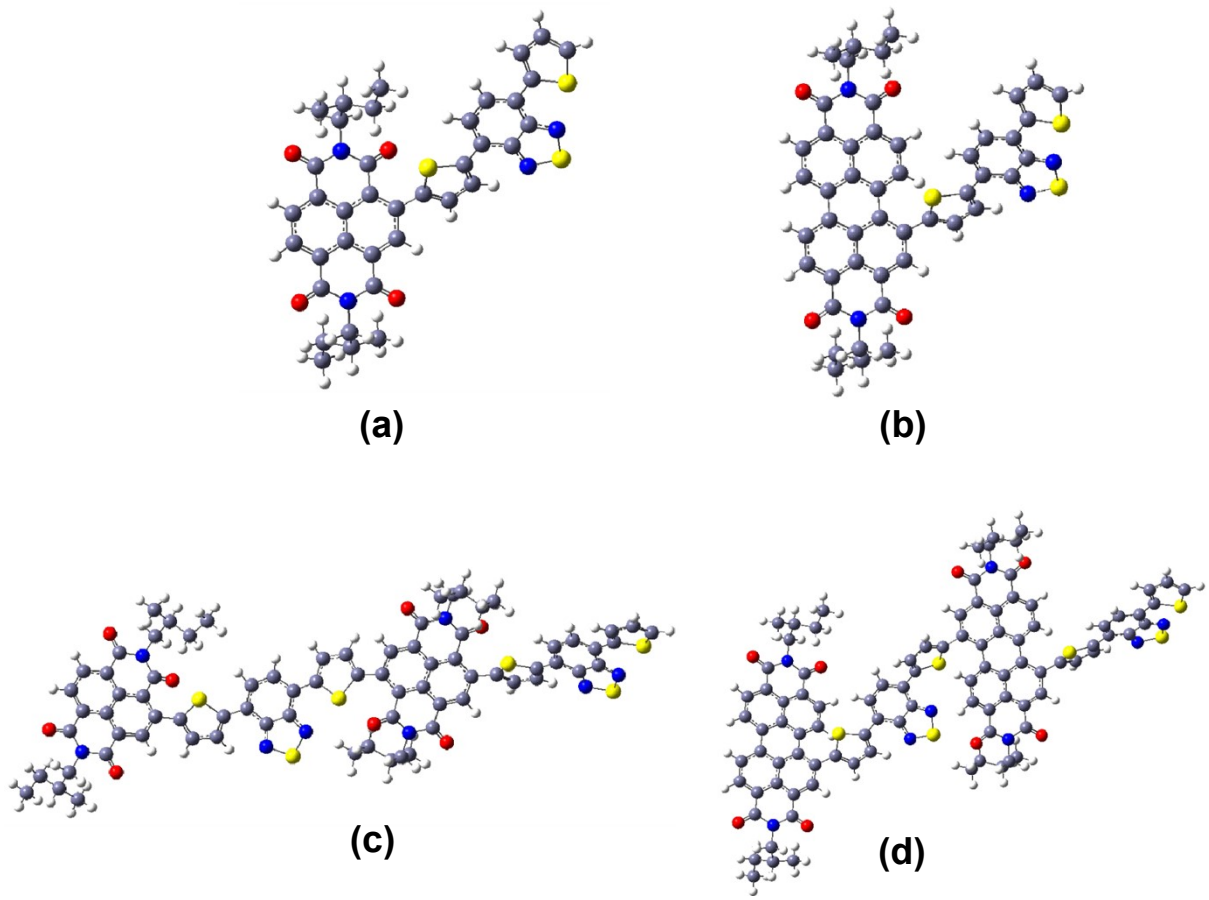

Supplementary Figure S7. The geometry-optimized structures of **BT-NDI** in (a) monomeric and (c) dimeric forms and **BT-PDI** in (b) monomeric and (d) dimeric forms, respectively.

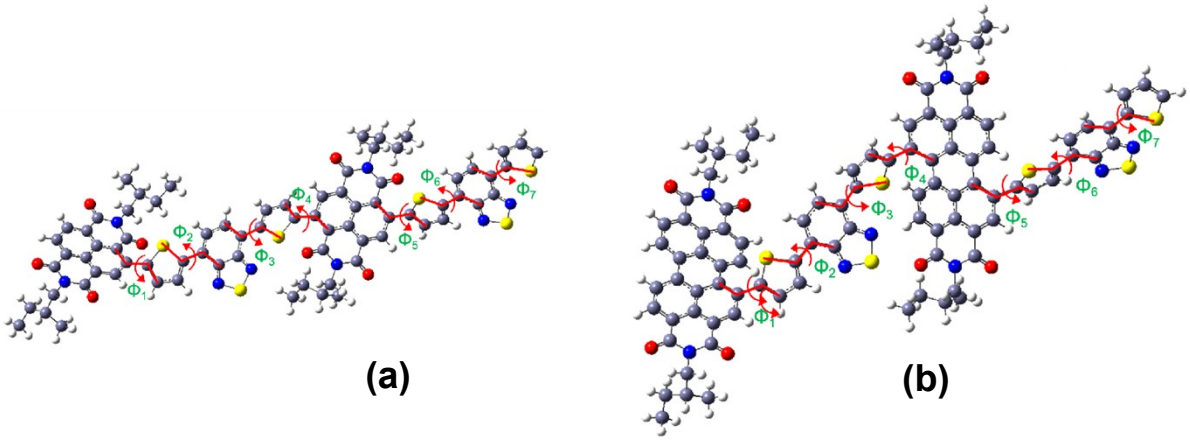

Supplementary Figure S8. Dihedral angles of the optimized geometries of (a) **BT-NDI** and (b) **BT-PDI** dimers. The dihedral angles between the junction of BT and NDI/PDI are defined by Φ1, Φ4, and Φ5 respectively. The NDI/PDI moiety remains planar in each monomer of the dimeric structure, while the BT moiety does not exhibit planarity.

Supplementary Table T3. Dihedrals of the optimized geometries of (a) **BT-NDI** and (b) **BT-PDI** dimers.

	Dihedral (in degree)	**BT-NDI**	**BT-PDI**
1	**Φ1**	135.1	130.5
2	Φ2	161.8	162.4
3	Φ3	157.2	137.1
4	**Φ4**	149.0	129.9
5	**Φ5**	134.1	123.7
6	Φ6	162.1	163.3
7	Φ7	163.0	162.0

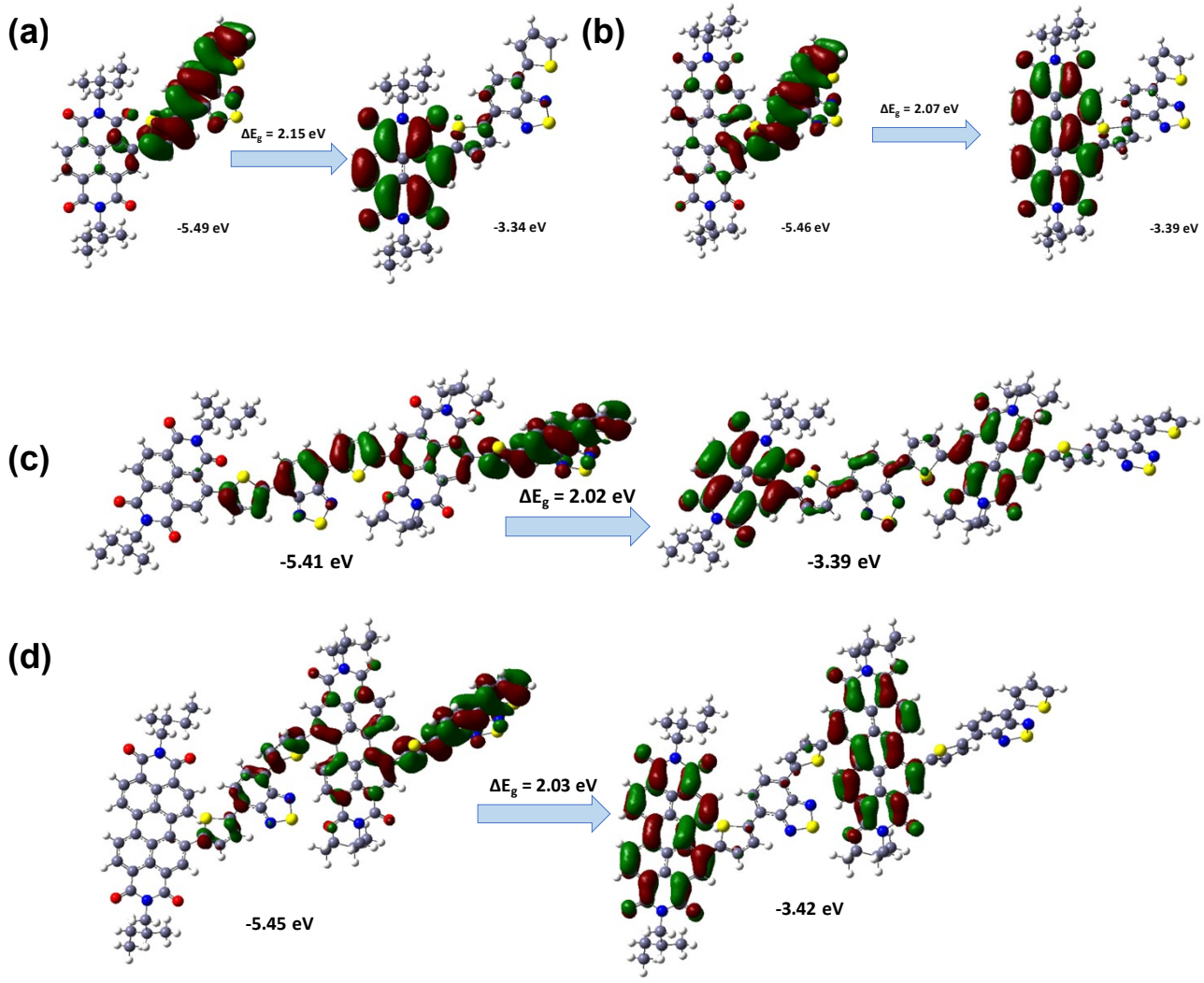

Supplementary Figure S9. The HOMO-LUMO energy diagrams of the monomeric units of (a) **BT-NDI** and (b) **BT-PDI** moieties, dimeric units of (c) **BT-NDI** and (d) **BT-PDI** moieties.

Supplementary Table T4. The HOMO and LUMO energy levels and the HOMO-LUMO energy gap (eV) for monomer, dimer, and trimer of **BT-NDI** and **BT-PDI**.

Energies are in eV	**BT-NDI**			**BT-PDI**		
	Monomer	Dimer	Trimer	Monomer	Dimer	Trimer
$\mathbf{E_{HOMO}}$	-5.49	-5.41	-5.39	-5.46	-5.45	-5.38
$\mathbf{E_{LUMO}}$	-3.34	-3.39	-3.41	-3.39	-3.42	-3.44
$\mathbf{\Delta E_g}$	2.15	2.02	1.98	2.07	2.03	1.94

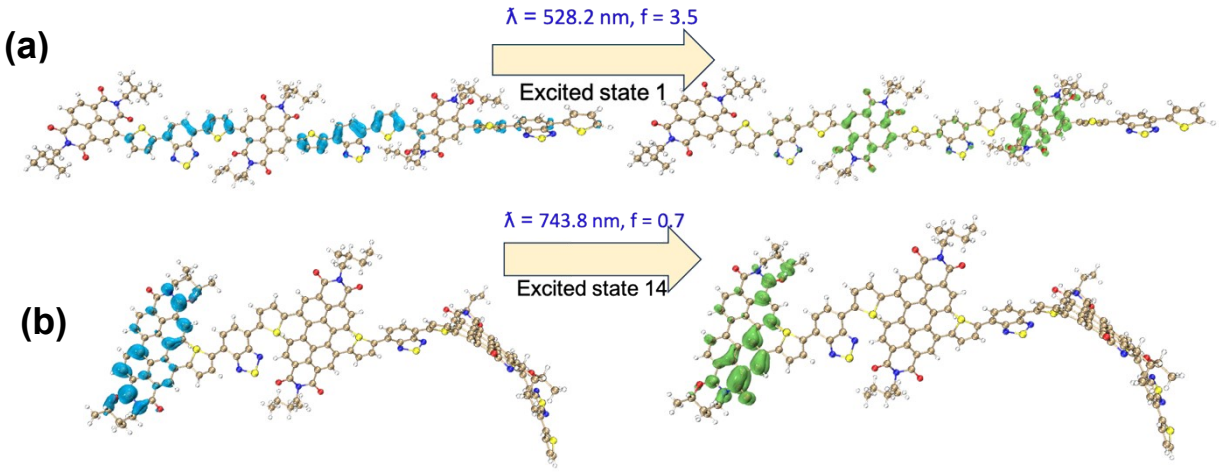

Supplementary Figure S10. Natural transition orbitals (NTO) corresponding to the characteristic UV-Vis absorption in the trimeric (a) **BT-NDI** and (b) **BT-PDI**. For each NTO, the hole (represented in blue colour) and electron (represented in green colour) orbitals are given in left and right, respectively. The transition wavelength (λmax) and the highest oscillator strength (f) for each transition are mentioned in the figure.

Supplementary Table T5. The absorption maxima (λ_{max}) corresponds to the characteristic UV-Vis absorption calculated from the TD-DFT method for the monomer, dimer, and trimer of **BT-NDI** and **BT-PDI**.

Absorption maxima (λ_{max})	**Monomer**	**Dimer**	**Trimer**
BT-NDI	290-474 nm	317-517 nm	316-528
BT-PDI	291-522 nm	306-542 nm	497-744

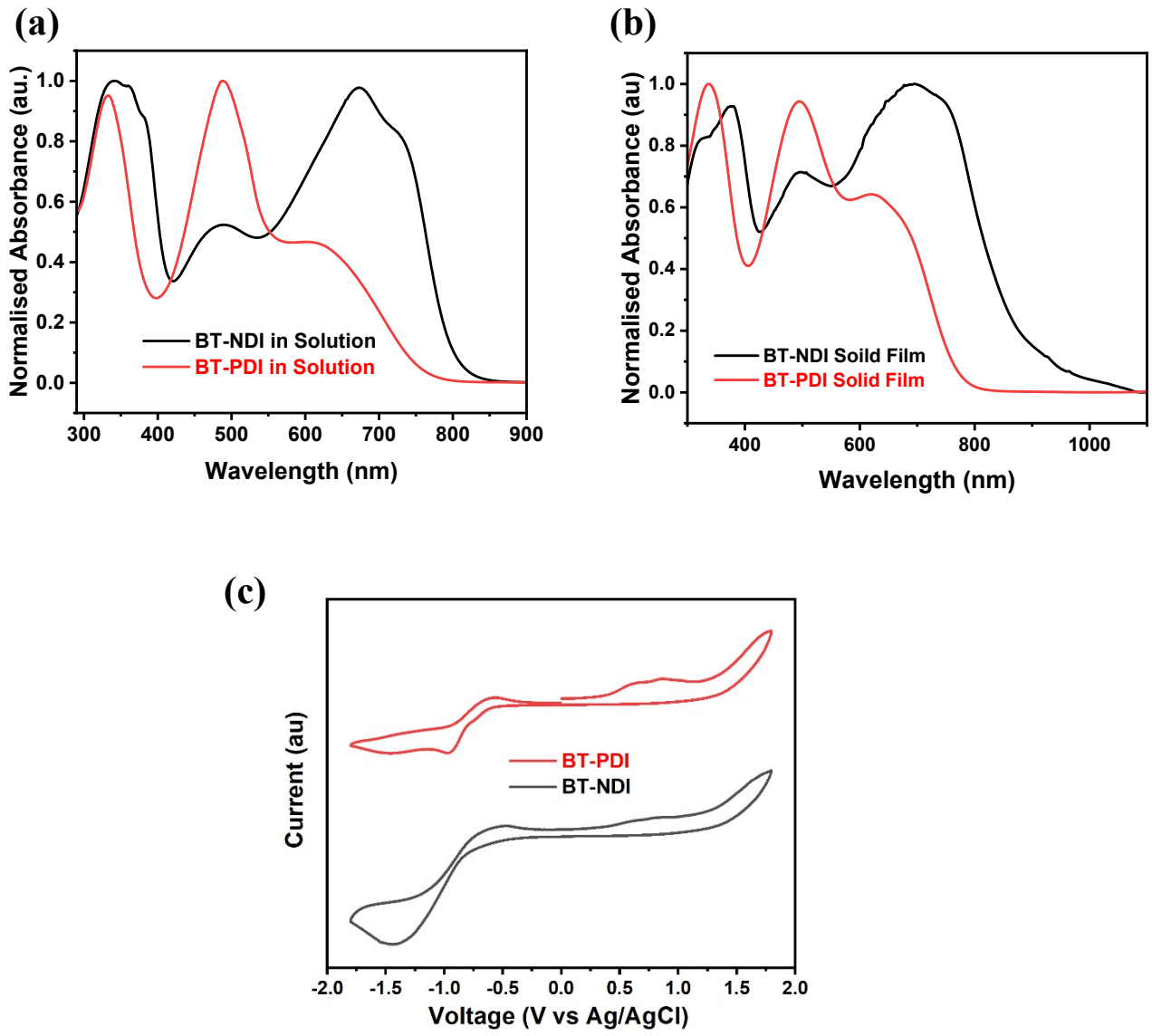

Supplementary Figure S11. Normalized UV-vis absorption spectra of **BT-NDI** and **BT-PDI**: (a) in a diluted chlorobenzene solution and (b) confined in thin films on glass substrates at room temperature. Cyclic voltammograms of **BT-NDI**, and **BT-PDI** in thin films (scan rate: 100 mV s^{-1})

Supplementary Table T6. Optical and electrochemical properties of **BT-NDI** and **BT-PDI**.

Semiconducting Polymer	[a]λ_{max}^{sol} (nm)	[b]λ_{max}Film (nm)	[c]HOMO (eV)	[c]LUMO (eV)	[d]E_g^{opt} (eV)	[e]E_g^{ec} (eV)
BT-NDI	341, 486, 676	367, 486, 681	−5.88	−3.77	1.41	2.11
BT-PDI	332, 491, 614	335, 496, 619	−5.80	−3.68	1.58	2.12

[a]Absorbance of copolymers in dilute chlorobenzene solution. [b]Spin-coated films of copolymers in chlorobenzene solution on glass surfaces. [c]$E_{HOMO}/E_{LUMO} = [-(E_{onset} - E_{onset\ (Fc/Fc^+\ vs.\ Ag/Ag+)}) - 4.8]$ eV, where 4.8 eV is the energy level of ferrocene below the vacuum level, and the formal potential, $E_{onset\ (Fc/Fc^+\ vs.\ Ag/Ag+)}$, is equal to 0.45 V. [d]Electrochemical band gap: $E_g^{ec} = E_{ox/onset} - E_{red/onset}$. Optical band gap: [d]$E_g^{opt} = 1240/\lambda_{edge}$.

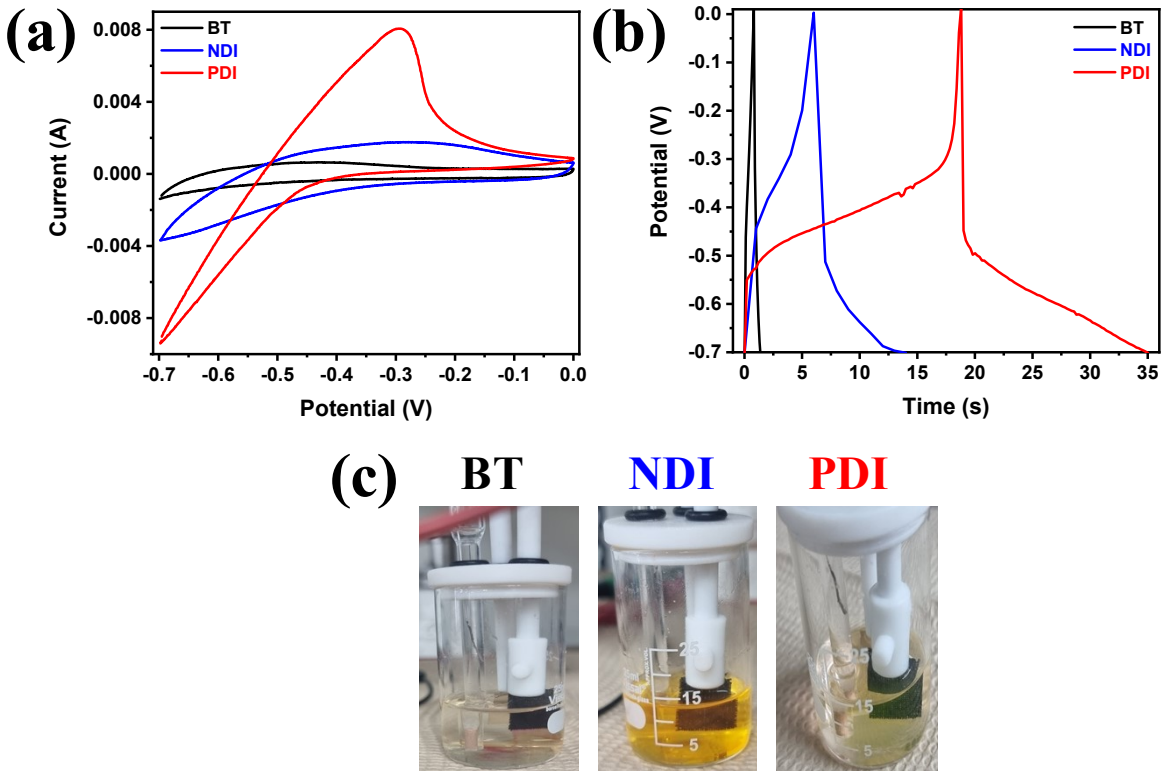

Supplementary Figure S12. (a) CV at 100 mV s^{-1} scan rate, (b) GCD at 1 A g^{-1} current density for the individual monomer units of BT, NDI and PDI, (c) Effect of applied current/potential on the monomeric working electrodes.

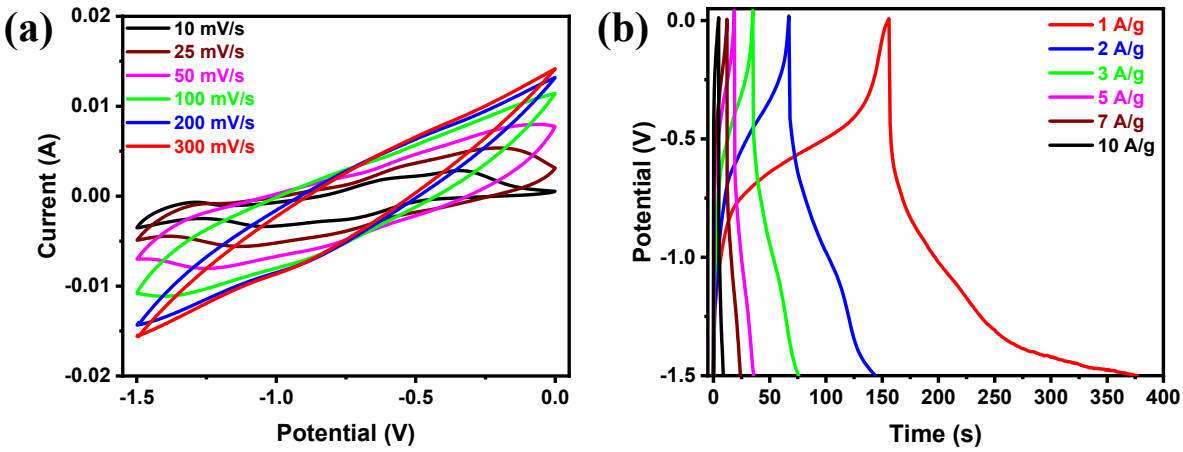

Supplementary Figure S13. (a) CV curves at different scan rates and (b) GCD curves at varying current densities for the **BT-NDI** polymeric electrode

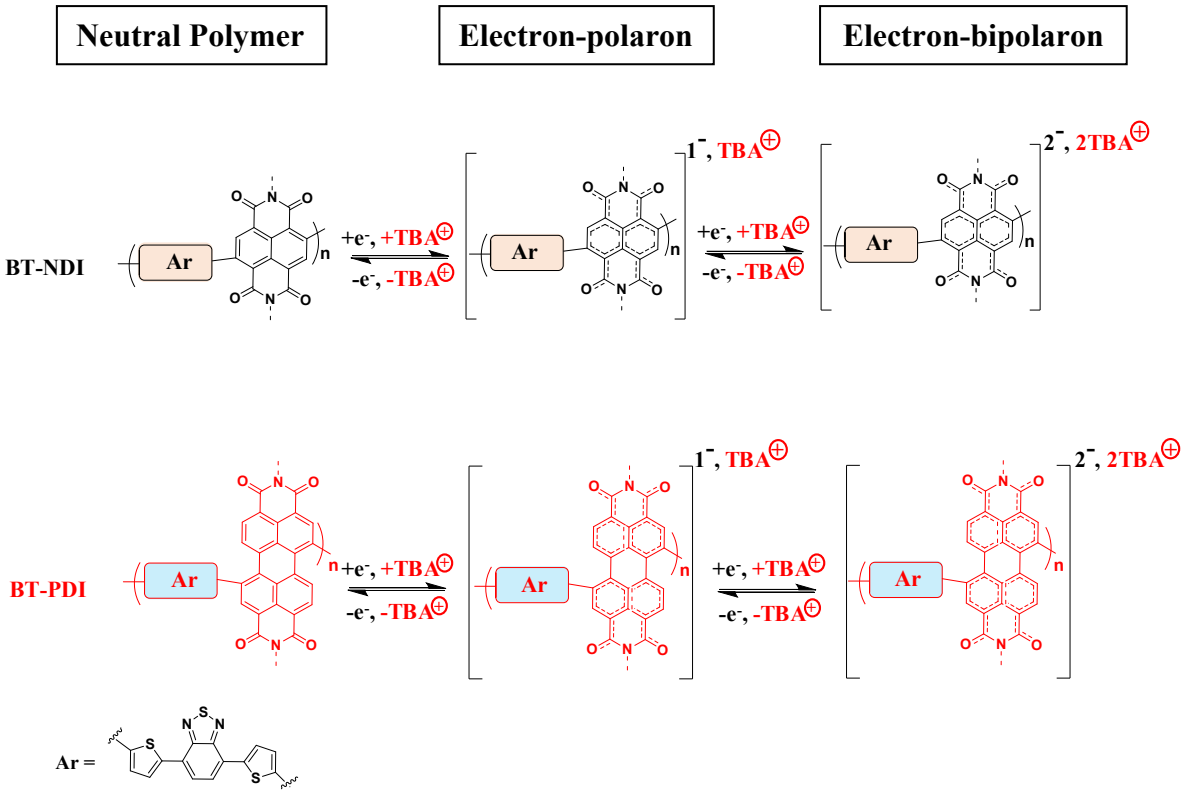

Supplementary Figure S14. Proposed plausible pseudocapacitive charge storage mechanism in the **BT-NDI** and **BT-PDI** conjugated polymers based on the reversible two consecutive one-electron reduction processes to form electron-polaron and electron-bipolaron.[S14-S15]

(S1) S. Sharma, R. Soni, S. Kurungot, S. K. Asha, *J. Phys. Chem. C* **2019**, *123*, 2084–2093.

(S2) Z. Chen, Y. Zheng, H. Yan, A. Facchetti, *J. Am. Chem. Soc.* **2009**, *131*, 8–9.

(S3) D. Patra, X. Zhan, R. Linthoinganbi, S. Muduli, S. Mishra, Y. Liu, S. Park, *J. Mater. Chem. C* **2023**, *11*, 1457–1463.

(S4) A. D. Becke, *J. Chem. Phys.* **1993**, *98*, 5648.

(S5) W. J. Hehre, R. Ditchfield, J. A. Pople, *J. Chem. Phys.* **1972**, *56*, 2257.

(S6) R. Ditchfield, W. J. Hehre, J. A. Pople, *J. Chem. Phys.* **1971**, *54*, 724.

(S7) L. A. Burns, Á. V.- Mayagoitia, B. G. Sumpter, C. D. Sherrill, *J. Chem. Phys.* **2011**, *134*, 084107.

(S8) T. Yanai, D. P. Tew, N. C. Handy, *Chem. Phys. Lett.* **2004**, *393*, 51-57.

(S9) M. J. Frisch, et al., Gaussian 09, *Gaussian, Inc., Wallingford CT*, **2016**.

(S10) T. Lu, F. Chen, *J. Comp. Chem.*, **2012**, 580-592.

(S11) W. Humphery, A. Dalke, K. Schulten, *J. Mol. Graph.* **1996**, *14*, 33-8, 27-8.

(S12) Z. Zhao, Z. Yin, H. Chen, L. Zheng, C. Zhu, L. Zhang, S. Tan, H. Wang, Y. Guo, Q. Tang, Y. Liu *Advanced Materials* **2017**, *29*, 1602410.

(S13) C. C. L. McCrory, S. Jung, J. C. Peters, T. F. Jaramillo, *Journal of the American Chemical Society* **2013,** *135,* 16977−16987.

(S14) A. A. Szumska et al., *Journal of the American Chemical Society* **2021,** *143,* 14795–14805.

(S15) Y. Cho, D. Jang, J. –J. Park, H. Kye, J. E. Kwon., B. -G. Kim, *ACS Appl. Energy Mater.,* **2023.**